

Supporting information

**Impregnation of metal ions in porphyrin-based imine gels to modulate
guest uptake and to assemble a catalytic microfluidic reactor**

Lihua Zeng, Peisen Liao, Haoliang Liu, Liping Liu, Ziwei Liang, Jianyong Zhang,* Liuping Chen
and Cheng-Yong Su

Sun Yat-Sen University, MOE Laboratory of Bioinorganic and Synthetic Chemistry, MOE Key

Laboratory of Polymeric Composite and Functional Materials, Lehn Institute of Functional

Materials, Guangzhou 510275, China. E-mail: zhjyong@mail.sysu.edu.cn

Experimental

Materials and methods

Chemicals and solvents were obtained from commercial sources and used as received without further purification. H_2tapp ,¹ Sn-tapp ,² Ni-tapp ,³ Pd-tapp ,⁴ tetrakis-(4-formylphenyl)methane⁵ and 1,3,5-benzenetricarboxaldehyde⁶ were synthesized as reported previously. Adsorption measurements were performed using a Quantachrome Autosorb-iQ2 analyzer. Prior to analysis, the aerogels were degassed at 100 °C for 16 h to remove solvent molecules. NMR spectra were obtained on a Bruker Avance III 400MHz or VARIAN Mercury-Plus 300 spectrometer. Solid state ^{13}C NMR spectrum was recorded on a Bruker AVANCE 400 Superconducting Fourier Transform Nuclear Magnetic Resonance Spectroscopy instrument. Scanning electron microscopy (SEM) and energy dispersive X-ray spectroscopy (EDX) were taken using a Quanta 400F scanning electron microscope with an Inca energy dispersive X-ray spectrometer or an Ultra-high Resolution FE-SEM SU8010 scanning electron microscope. Before measurement, the aerogel sample was dispersed in ethanol with the aid of sonication, put on aluminum foil, and sputter coated with gold. Transmission electron microscopy (TEM) investigations were carried out on a FEI Tecnai G2 Spirit 120 kV transmission electron microscope. The aerogel sample was dispersed in ethanol with the aid of sonication and mounted on a carbon coated copper grid. X-ray powder diffraction data were collected on a Bruker Smartlab diffractometer at 40 kV and 30 mA with a Cu-target tube. Thermo analyses were performed under N_2 atmosphere at a heating rate of 10 °C min^{-1} with a NETZSCH TG STA 449 F3 Jupiter system. MS experiments were performed on a Bruker MALDI-TOF-TOF ultrafleXtreme mass spectrometer. UV/Vis spectra were measured on a SHIMADZU-2450 spectrophotometer. Metal analyses were performed by inductively coupled plasma atomic emission spectroscopy using a TJA IRIS HR% ICP instrument. To prepare the samples for ICP-AES, a dry-ashing method with HNO_3 was used to digest the aerogel.

Synthesis of Fe-tapp

FeCl₂·4 H₂O (475.0 mg, 2.40 mmol) was added into H₂tapp (135.0 mg, 0.20 mmol) in DMF (20 mL) upon refluxing under argon atmosphere. After 6 h, the reaction was carried on in air. 2 h later, the reaction mixture was cooled down to RT and filtered. 30 mL H₂O was added into the filtrate and the precipitate was filtered and washed with water and ethanol three times respectively. The crude product was recrystallized from DMF-water to obtain dark red solid (88.0 mg, 56%). Microanal. found (calcd.) for C₄₄H₃₂N₈FeCl·1.5H₂O: C 66.93 (66.80), H 4.84 (4.46), N 13.88 (14.16)%. UV-vis: λ_{max} = 421.5 nm (DMF). TOF-MS (MALDI+): *m/z* found (calcd.) for [M-Cl]⁺ ([C₄₄H₃₂N₈Fe]⁺) = 728.215 (728.209).

Synthesis of Mn-tapp

Mn(OAc)₂·4H₂O (367.5 mg, 1.50 mmol) was added into H₂tapp (202.5 mg, 0.30 mmol) in DMF (10 mL) upon refluxing. After 30 min, the reaction was cooled to RT and saturated aqueous NaCl solution (10 mL) was added. The resulting mixture was stirred at room temperature overnight and filtered. The solid was filtered and washed with water and ethanol three times respectively. The crude product was recrystallized from DMF-water and washed by EtOH, then dried under vacuum to obtain dark green solid (151.1 mg, 66%). Microanal. found (calcd.) for C₄₄H₃₂N₈MnCl: C 68.84 (69.25), H 4.32 (4.23), N 14.36 (14.68%) UV-vis: λ_{max} = 476.5 nm (DMF). TOF-MS (MALDI+): *m/z* found (calcd.) for [M-Cl]⁺ ([C₄₄H₃₂N₈Mn]⁺) = 727.215 (727.212).

Preparation of porphyrin imine gels/aerogels

Typical procedure: To a solution of H₂tapp (20.2 mg, 0.03 mmol) in DMSO (0.5 mL), a solution of tetrakis-(4-formylphenyl)methane (12.9 mg, 0.03 mmol) in DMSO (0.5 mL) was added dropwise whilst stirring to form a solution. To the solution mixture, HOAc (30 μL, 3 mol L⁻¹ in DMSO) was added. The resulting solution was heated in a closed vial at 80 °C to obtain an opaque gel. The resulting gel was further aged for 24 h. The gel was subsequently washed with DMSO at RT. DMSO was replaced every day by fresh solvent

and solvent exchange was finished after three days. Then the gel was washed with anhydrous EtOH for three days in similar way. The solvent in the exchanged gel was next extracted with subcritical CO₂(l) (270 g) for 20 h in a 0.75 L high pressure stainless-steel Soxhlet extractor and the extraction temperature was kept at 35 °C (pressure 5.8 MPa). After the stainless-steel autoclave was depressurized slowly at RT for about 2-3 h H₂tapp-**A4** aerogel was obtained (27.7 mg, 89%).

Gel capillary reactor

Prior to the coating of Pd-tapp-**A4** gel, the inner surface of a silica capillary column (L = 3.0 m, ID = 0.53 mm) was modified with amino groups.⁶ First the capillary was rinsed with acetone, 1% NaOH aqueous solution, distilled water and 0.1% HCl aqueous solution for 30 min respectively. After that the capillary was rinsed with ethanol and dry toluene for 10 min, respectively. Subsequently the capillary was filled with a solution of 3-aminopropyl-siloxyethane in dry toluene (1% v:v) and kept in 80 °C for 12 h. Afterwards this solution was removed and the capillary was rinsed with dry toluene and EtOH for 10 min, respectively, and dried in a stream of argon for 4 h.

The above pre-treated capillary was filled with the solution mixture of a solution of Pd-tapp (23.4 mg, 0.03 mmol) in DMSO (0.5 mL), a solution of tetrakis-(4-formylphenyl)methane (**A4**) (12.9 mg, 0.03 mmol) in DMSO (0.5 mL), and HOAc (30 µL, 3 mol L⁻¹ in DMSO). The capillary was sealed and kept for 15 min at room temperature. Then the solution was removed by flushing the capillary with argon and the capillary was flushed with argon for 30 min. The capillary was sealed and heated at 80 °C for 24 h. The capillary was rinsed with DMSO (1 mL × 3). The procedures were repeated for five times to obtain a capillary for catalytic study (the coating thickness was ca. 2 µm according to SEM). Prior to catalysis, DMSO solvent in the gel was exchanged to DMF.

Suzuki-Miyaura cross-coupling reaction in gel capillary reactor

In a typical process, a substrate solution was prepared by dissolving 4-bromoanisole (93.5 mg, 0.50 mmol), phenylboronic acid (91.5 mg, 0.75 mmol) and CsF (182.3 mg, 1.20 mmol)

in DMF-H₂O (10 mL, v:v = 1:1). An aliquot (50 µL) of the substrate solution was injected into a continuous flow of DMF-H₂O (10 mL, v:v = 1:1) through a Rheodyne 7725 injector port, then injected into the gel capillary reactor that is heated to 100 °C in an oil bath. The liquid flow rate was set at 10 µL min⁻¹ by using a New Era NE-4000 syringe pump. After a residence time period of 30 min from the initial substrate injection the product was flushed off the capillary reactor by using a higher flow of DMF-H₂O (10 mL, v:v = 1:1) (200 µL min⁻¹). The product was collected during a period of ca. 1 min. Then Et₂O was added to the mixture, and the organic layer was subjected to GC analysis. For subsequent use, the capillary reactor was rinsed with DMF-H₂O (1 mL, v:v = 1:1) for three times.

Suzuki-Miyaura cross-coupling reaction under batch conditions

In a typical process, to the solution mixture of 4-bromoanisole (93.5 mg, 0.50 mmol), benzenboronic acid (91.5 mg, 0.75 mmol) and CsF (182.3 mg, 1.20 mmol) in DMF-H₂O (10 mL, v:v = 1:1), Pd-tapp-A4 gel catalyst (0.005 mmol, 1 mol%) was added. The resulting reaction mixture was heated at 100 °C. For recovering, the gel catalyst was separated by centrifugation and washed by water and DMF in sequence.

Calculation of isosteric heats of gas adsorption Q_{st}

The isosteric heats of gas adsorption Q_{st} were calculated from the Clausius-Clapeyron equation using the virial-type equation:⁷

$$y = \ln x + \frac{1}{T} \sum_{i=0}^7 a_i x^i + \sum_{i=0}^4 b_i x^i$$

where y is the logarithmic function of relative pressure, $y = \ln(P/P_0)$, while x and T are the amount adsorbed (mmol g⁻¹) and temperature (K) respectively, and a_i and b_i are empirical parameters. Parameters a_i and b_i are obtained by fitting this equation to the adsorption data measured at 273 K and 298 K. The isosteric heat of adsorption as a function of x is calculated following Clausius-Clapeyron equation:

$$Q_{st} = -R \times \sum_{i=0}^7 a_i x^i$$

where R is the universal gas constant.

The Q_{st} curves were estimated by applying the virial equation to the gas isotherms at 273 and 298 K.

- 1 A. Bettelheim, B. A. White, S. A. Raybuck and R. W. Murray, *Inorg. Chem.*, 1987, **26**, 1009-1017.
- 2 (a) A. D. Adler, F. R. Longo, F. Kampas and J. Kim, *J. Inorg. Nucl. Chem.*, 1970, **32**, 2443-2445; (b) F. Zadehahmadi, F. Ahmadi, S. Tangestaninejad, M. Moghadam, V. Mirkhani, I. M. Baltork and R. Kardanpour, *J. Mol. Catal. A Chem.*, 2015, **398**, 1-10.
- 3 W. Meng, B. Breiner, K. Rissanen, J. D. Thoburn, J. K. Cleggand and J. R. Nitschke, *Angew. Chem.*, 2011, **123**, 3541-3545.
- 4 V. A. Ol'shevskaya, A. V. Zaitsev, Y. V. Dutikova, V. N. Luzgina, E. G. Kononova, P. V. Petrovsky and V. N. Kalinin, *Macroheterocycles*, 2009, **2**, 221-227.
- 5 J. H. Fournier, X. Wang and J. D. Wuest, *Can. J. Chem.*, 2003, **81**, 376-380.
- 6 P. Pandey, A. P. Katsoulidis, I. Eryazici, Y. Y. Wu, M. G. Kanatzidis and S. T. Nguyen, *Chem. Mater.*, 2010, **22**, 4974-4979.
- 7 (a) I. I. Salame and T. J. Bandosz, *Langmuir*, 2000, **16**, 5435-5440; (b) C. Petit, L. Huang, J. Jagiello, J. Kenvin, K. E. Gubbins and T. J. Bandosz, *Langmuir*, 2011, **27**, 13043-13051.

Table S1. Preparation of various porphyrin imine gels in DMSO (gelation temperature, 80 °C; -NH₂ : -CHO = 1:1; *c*_{tapp} = 0.030 mol L⁻¹, HOAc (cat.) 0.009 mmol).

Entry	Composition	Time/h	Result
1	H ₂ tapp- A2	2.0	opaque purple gel
2	H ₂ tapp- A3	0.5	opaque purple gel
3	H ₂ tapp- A4	4.0	opaque purple gel
4	Pd-tapp- A4	0.5	opaque dark red gel
5	Ni-tapp- A4	0.5	opaque dark red gel
6	Mn-tapp- A4	8.0	opaque green gel
7	Fe-tapp- A4	2.0	opaque brown gel
8	Sn-tapp- A4	4.0	opaque dark green gel

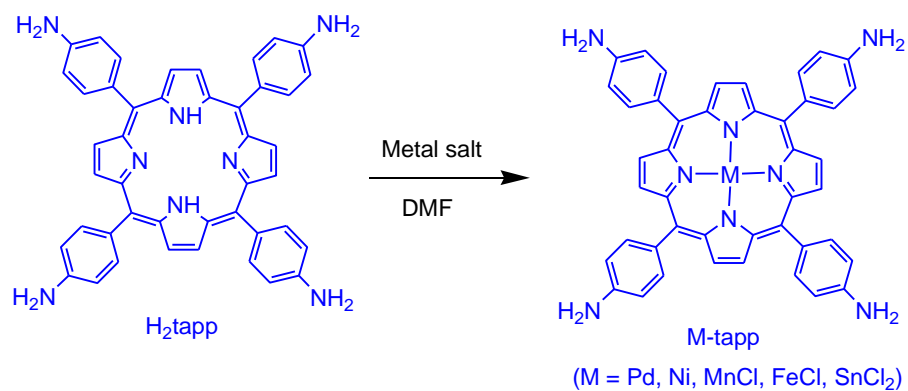
Table S2. Elemental analyses of various aerogels.

Aerogel	Formula	C%	H%	N%	Metal%
		Found/cal.	Found/cal.	Found/cal.	Found/cal.
H ₂ tapp- A4	C ₇₃ H ₄₆ N ₈	84.36/84.70	4.51/4.48	10.98/10.82	----
Pd-tapp- A4	C ₇₃ H ₄₄ N ₈ Pd·9H ₂ O	67.62/67.36	4.40/4.80	8.76/8.61	8.36/8.17
Ni-tapp- A4	C ₇₃ H ₄₄ N ₈ Ni	79.93/80.30	4.09/4.06	10.58/10.26	4.93/5.38
Mn-tapp- A4	C ₇₃ H ₄₄ N ₈ MnCl	78.11/78.04	4.27/3.95	10.18/9.97	4.56/4.89
Fe-tapp- A4	C ₇₃ H ₄₄ N ₈ FeCl·0.25H ₂ O	77.41/77.66	4.47/3.97	10.22/9.92	4.50/4.95
Sn-tapp- A4	C ₇₃ H ₄₄ N ₈ SnCl ₂ ·10H ₂ O	62.67/62.50	4.18/4.60	7.71/7.99	9.08/8.46

Table S3. Catalytic performance of Pd-tapp-**A4** gel in the gel capillary reactor (substrates have 30 min residence time, ID 0.53 mm × 1000 mm) at 100 °C for five runs of Suzuki-Miyaura reaction of 4-bromoanisole and phenylboronic acid.

run	1	2	3	4	5
yield/% ^a	85	85	85	84	82

^a Determined by GC.



Scheme S1. Synthetic route of M-tapp (M = Pd, Ni, MnCl, FeCl and SnCl₂). Metal salts: PdCl₂, NiCl₂·6H₂O, Mn(OAc)₂·4H₂O, FeCl₂·4H₂O and SnCl₂·2H₂O.

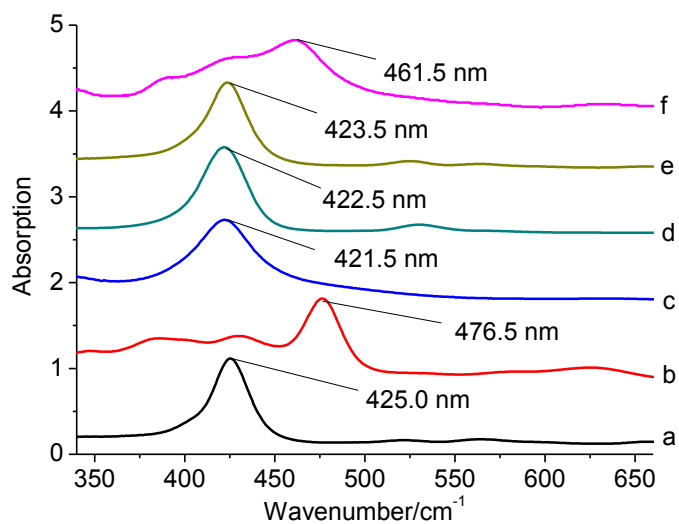


Figure S1. UV-vis absorption spectra of a) H₂tapp, b) Mn-tapp, c) Fe-tapp, d) Ni-tapp, e) Pd-tapp and f) Sn-tapp in DMF.

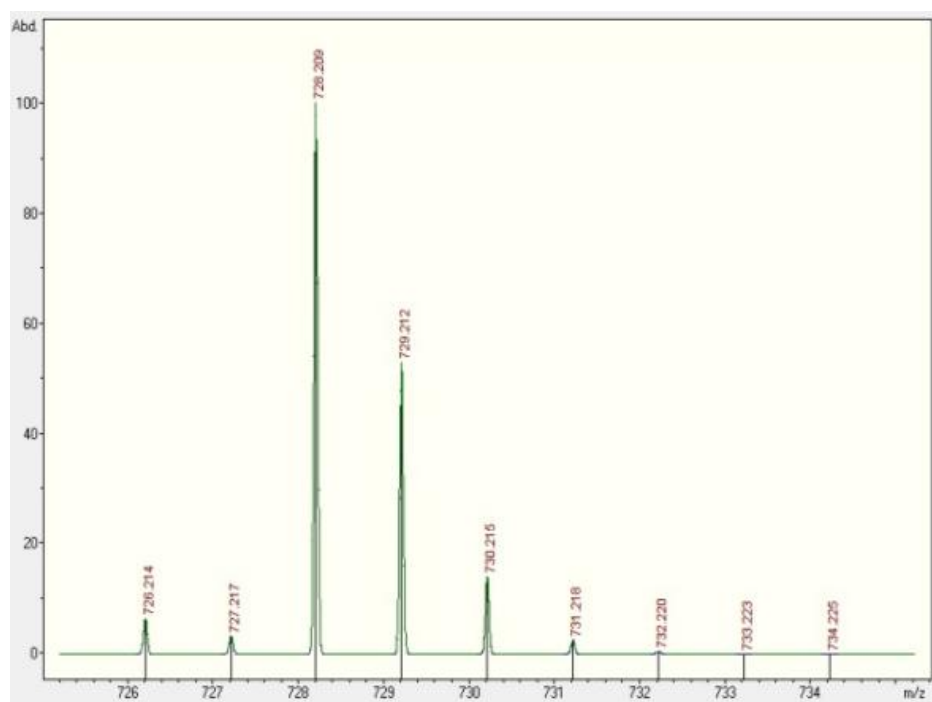
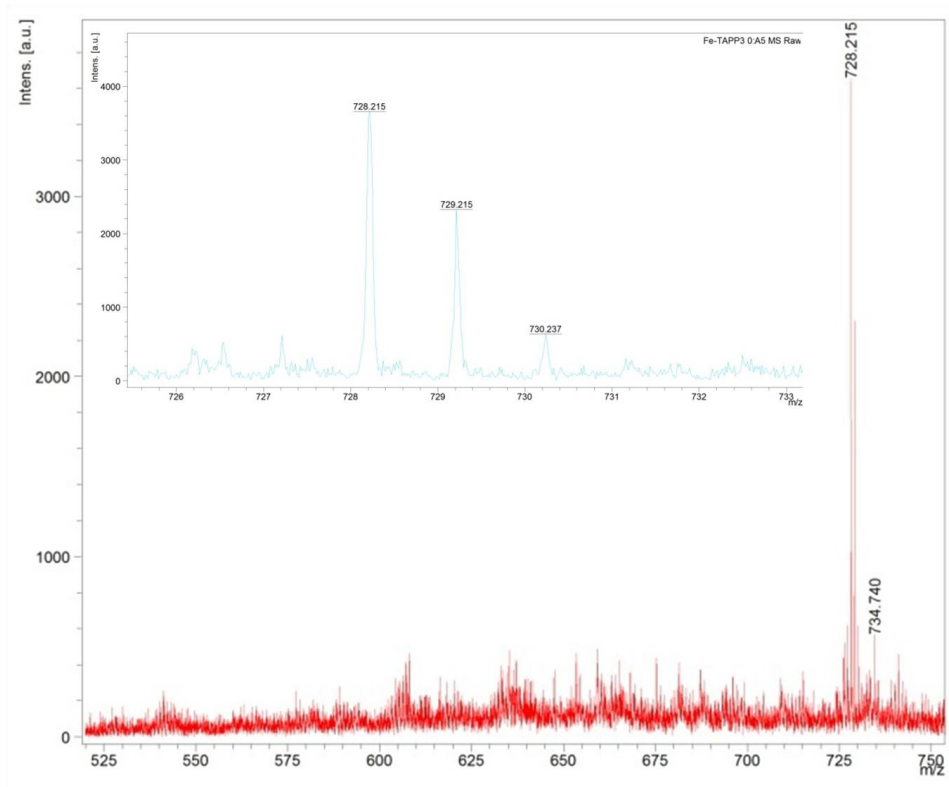


Figure S2. The MALDI-MS spectrum of Fe-tapp, and isotopic distribution and simulation of $[M-Cl]^+$ ($[C_{44}H_{32}N_8Fe]^+$).

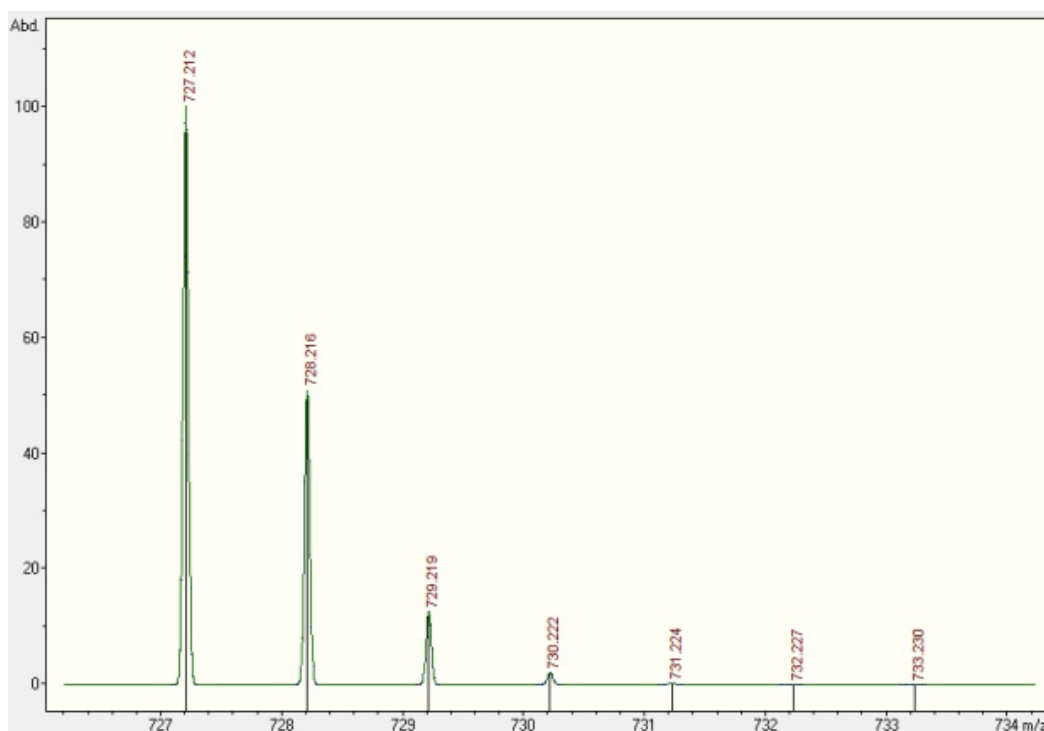
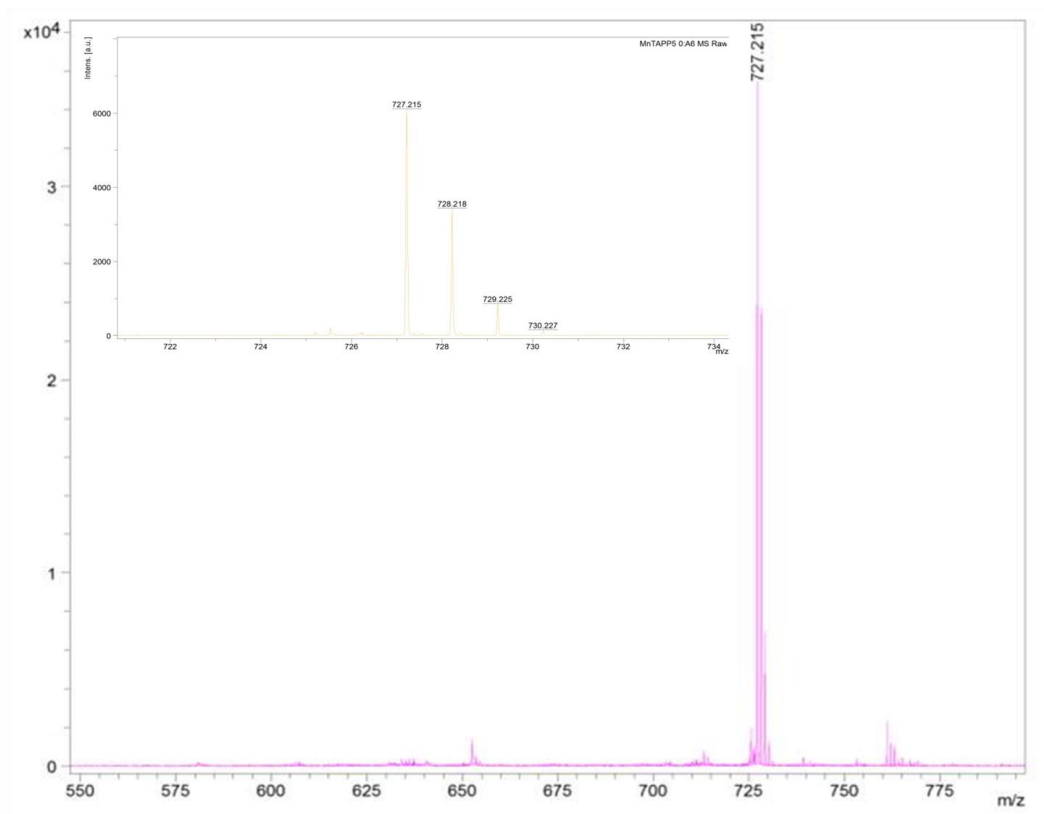


Figure S3. The MALDI-MS spectrum of Mn-tapp, and isotopic distribution and simulation of $[M-Cl]^+$ ($[C_{44}H_{32}N_8Mn]^+$).

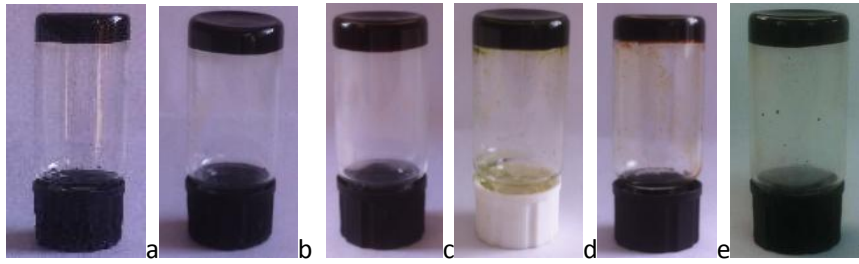


Figure S4. Photographic images of imine wet gels, a) H₂tapp-A2, b) H₂tapp-A3, c) Ni-tapp-A4, d) Mn-tapp-A4, e) Fe-tapp-A4 and f) Sn-tapp-A4.

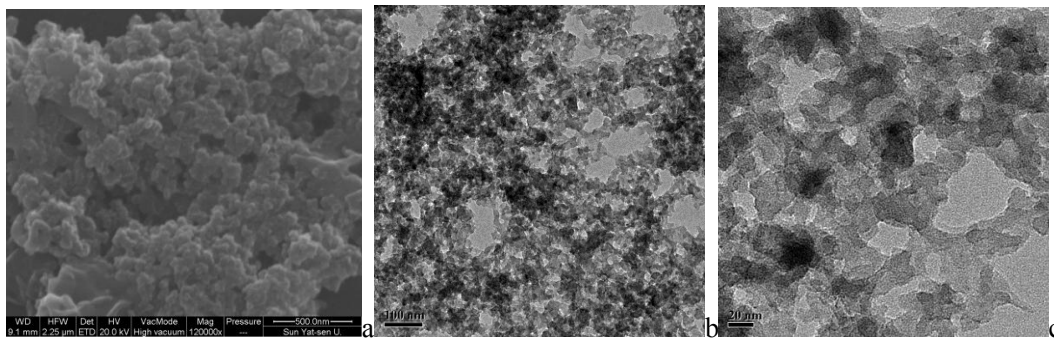


Figure S5. a) SEM and b,c) TEM images of H₂tapp-A2 aerogel (bars represent 500, 100 and 20 nm from left to right).

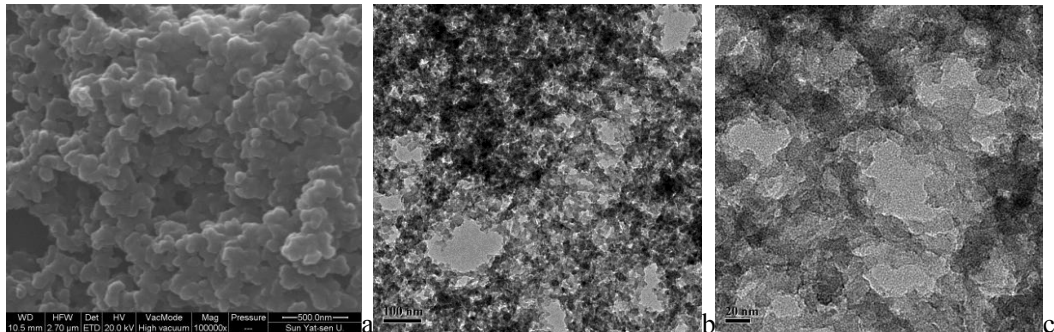


Figure S6. a) SEM and b,c) TEM images of H₂tapp-A3 aerogel (bars represent 500, 100 and 20 nm from left to right).

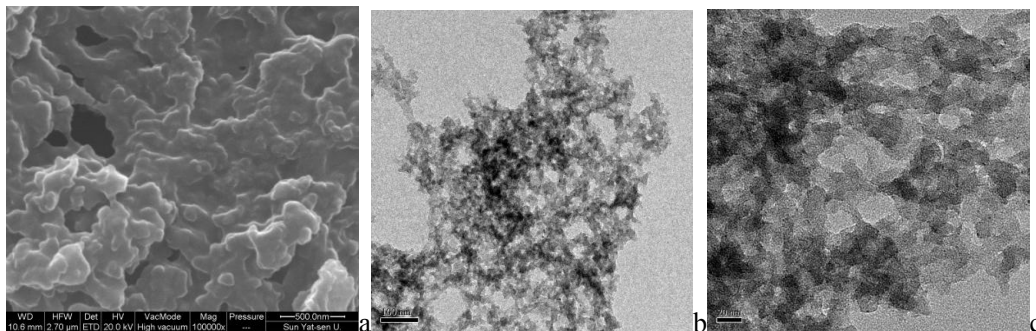


Figure S7. a) SEM and b,c) TEM images of Ni-tapp-A4 aerogel (bars represent 500, 100 and 20 nm from left to right).

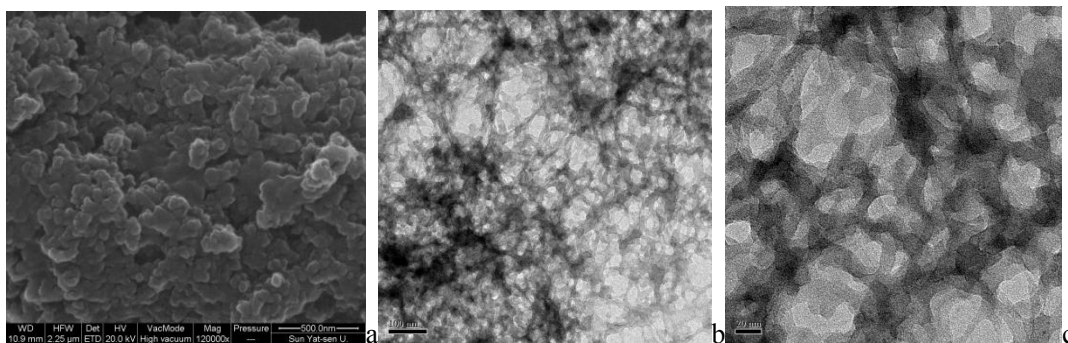


Figure S8. a) SEM and b,c) TEM images of Mn-tapp-A4 aerogel (bars represent 500, 100 and 20 nm from left to right).

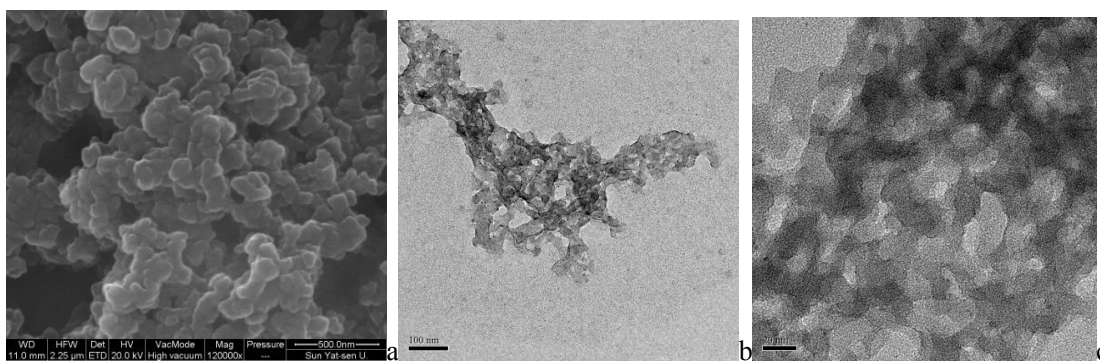


Figure S9. a) SEM and b,c) TEM images of Fe-tapp-A4 aerogel (bars represent 500, 100 and 20 nm from left to right).

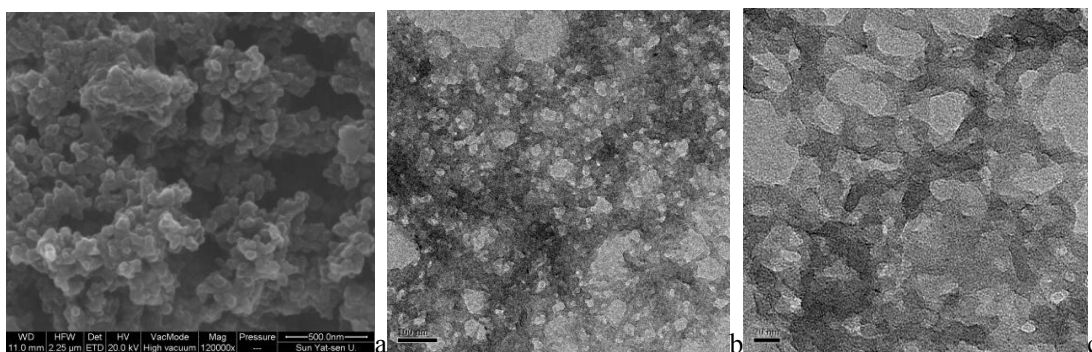


Figure S10. a) SEM and b,c) TEM images of Sn-tapp-A4 aerogel (bars represent 500, 100 and 20 nm from left to right).

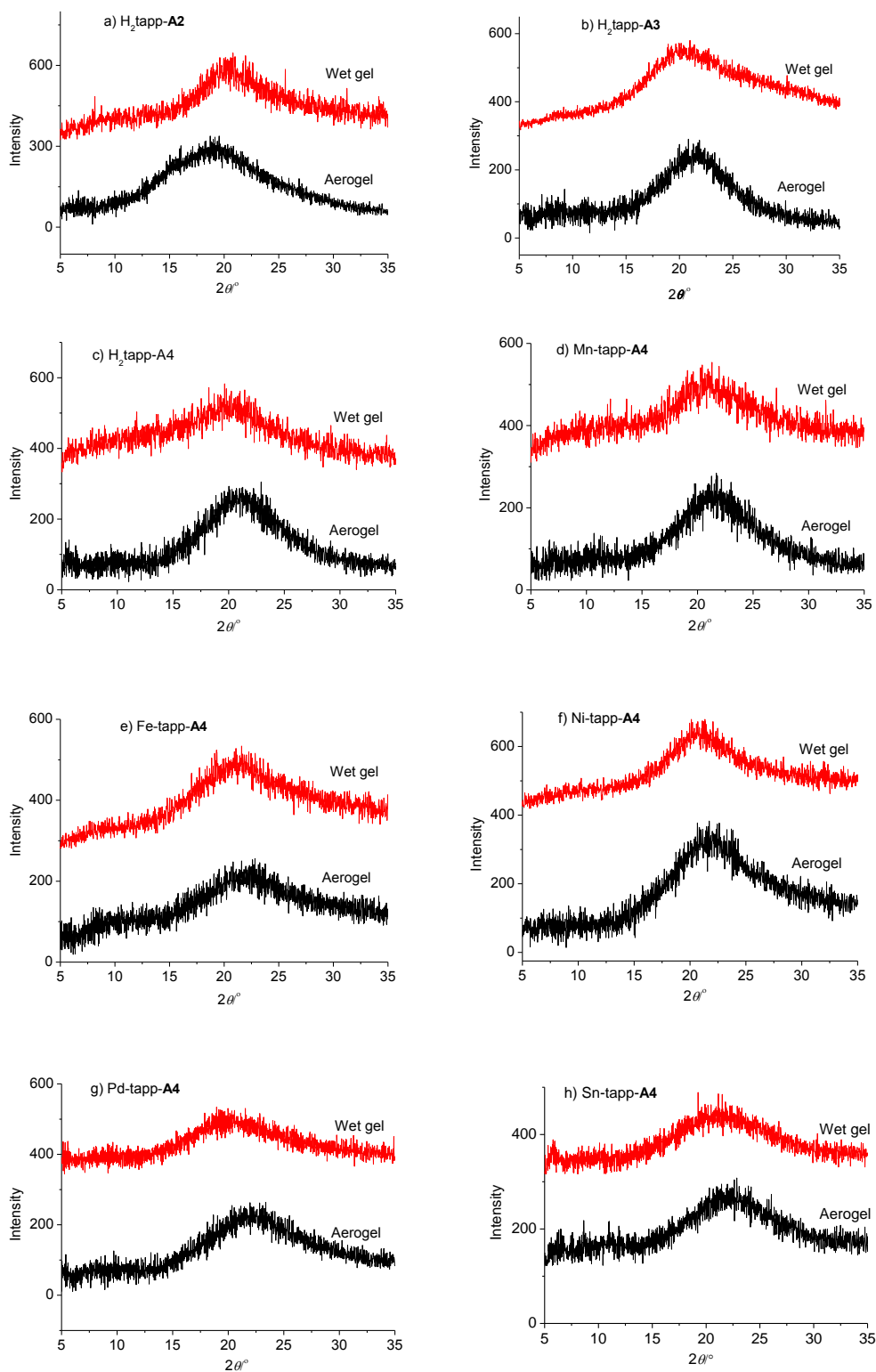


Figure S11. XRPD patterns of a) $\text{H}_2\text{tapp-A2}$, b) $\text{H}_2\text{tapp-A3}$, c) $\text{H}_2\text{tapp-A4}$, d) Mn-tapp-A4 , e) Fe-tapp-A4 , f) Ni-tapp-A4 , g) Pd-tapp-A4 and h) Sn-tapp-A4 wet gels and aerogels. The patterns of wet gels are vertically offset for clarity.

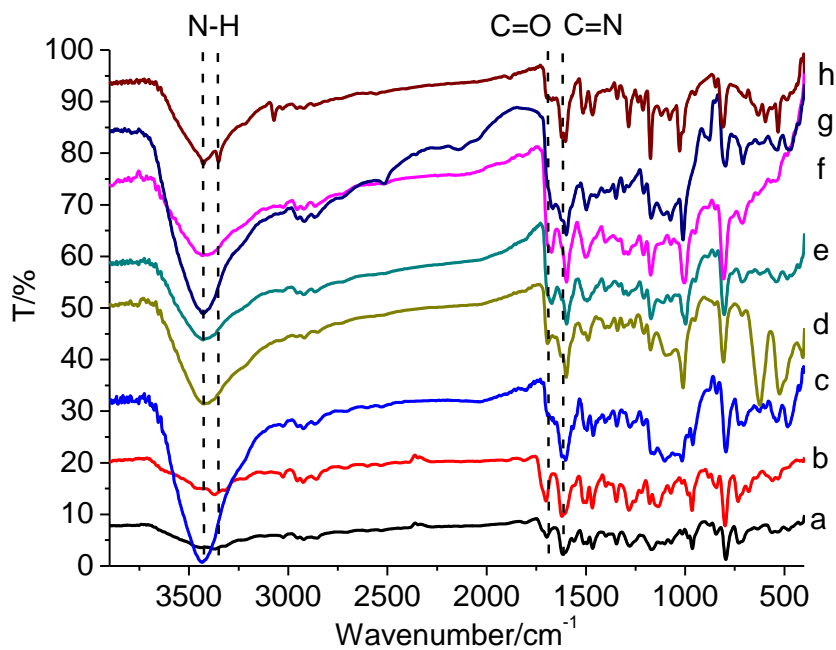


Figure S12. FT-IR spectra of a) H₂tapp-A2, b) H₂tapp-A3, c) H₂tapp-A4, d) Mn-tapp-A4, e) Fe-tapp-A4, f) Ni-tapp-A4, g) Pd-tapp-A4 and h) Sn-tapp-A4 aerogels. The spectra are vertically offset for clarity.

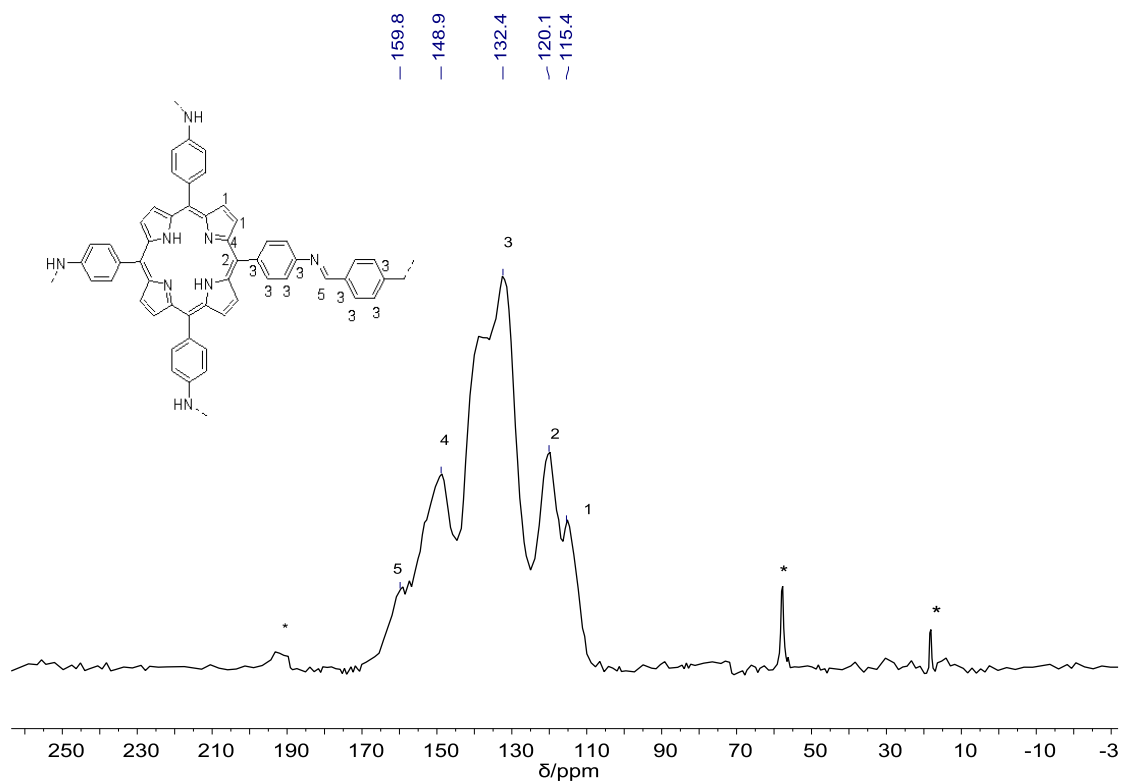


Figure S13. Solid-state ¹³C CP/MAS NMR spectrum of H₂tapp-A2 aerogel. Signals with * symbols are spinning sidebands.

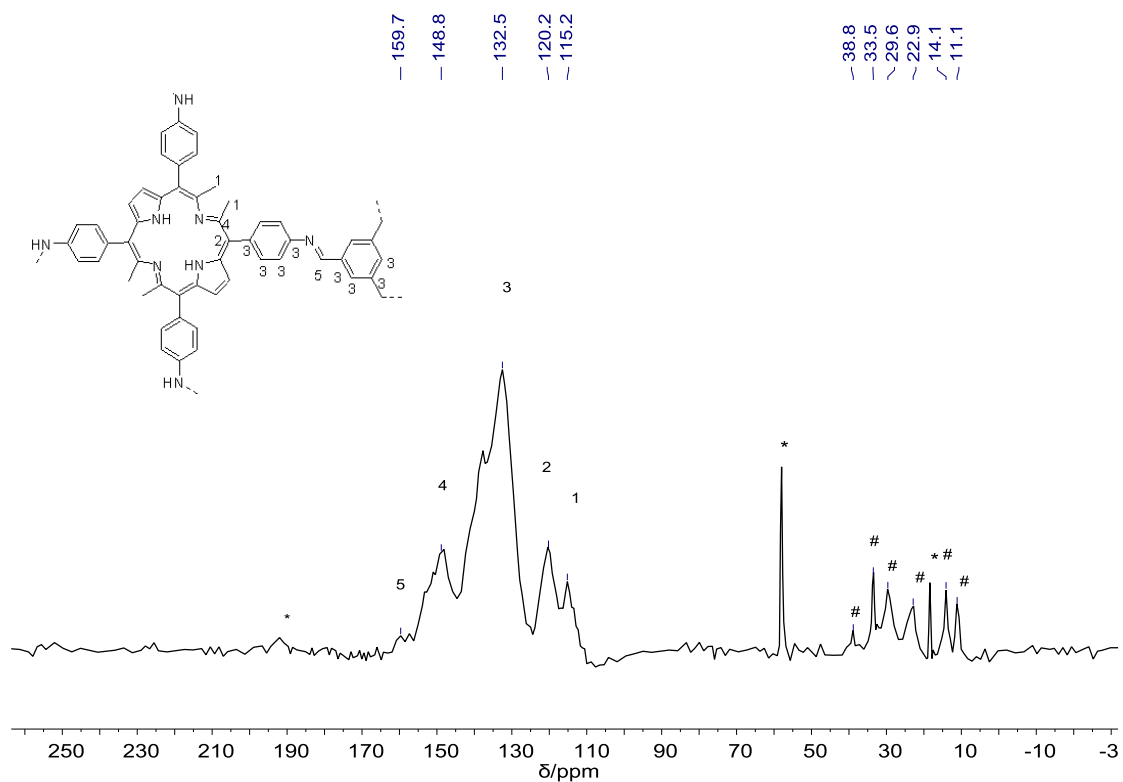


Figure S14. Solid-state ^{13}C CP/MAS NMR spectrum of H₂tapp-A3 aerogel. Signals with * symbols are spinning sidebands, and signals with # symbols are due to residue solvents.

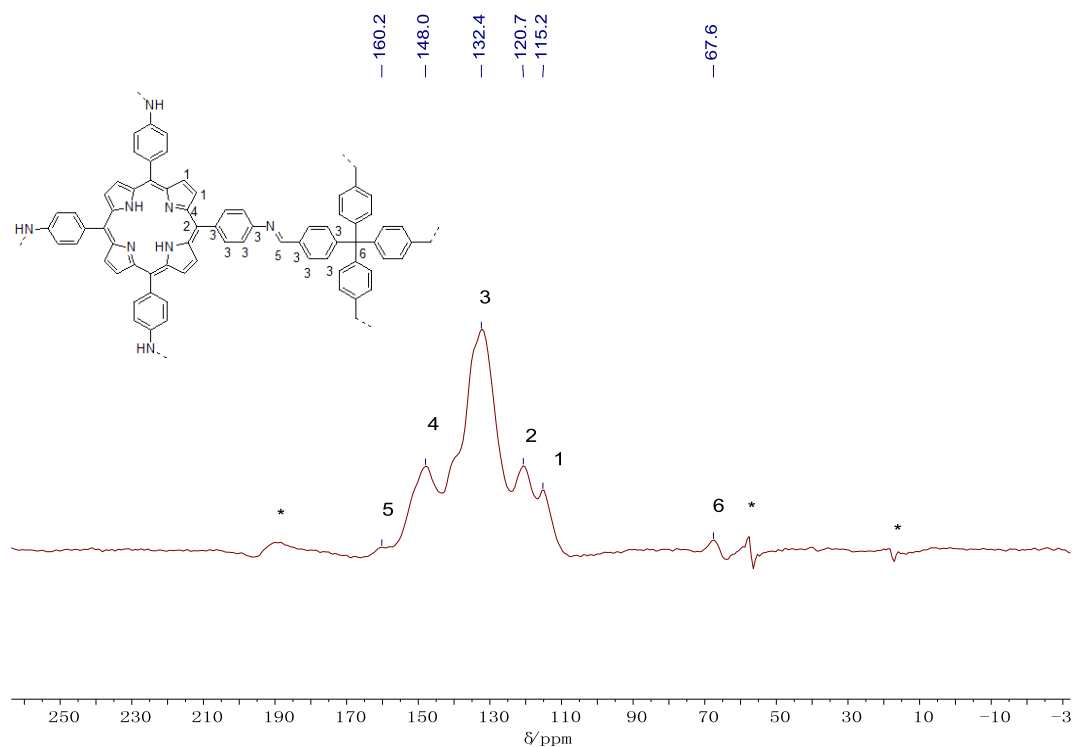


Figure S15. Solid-state ^{13}C CP/MAS NMR spectrum of H₂tapp-A4 aerogel. Signals with * symbols are spinning sidebands.

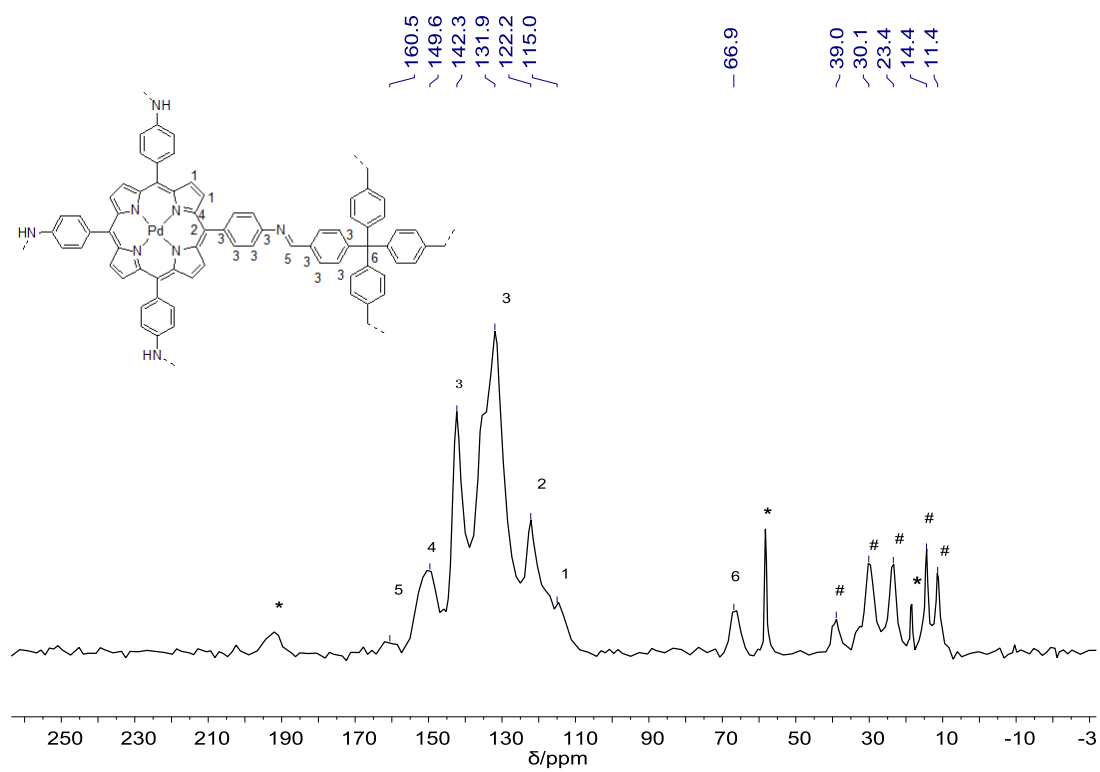


Figure S16. Solid-state ^{13}C CP/MAS NMR spectrum of Pd-tapp-A4 aerogel. Signals with * symbols are spinning sidebands, and signals with # symbols are due to residue solvents.

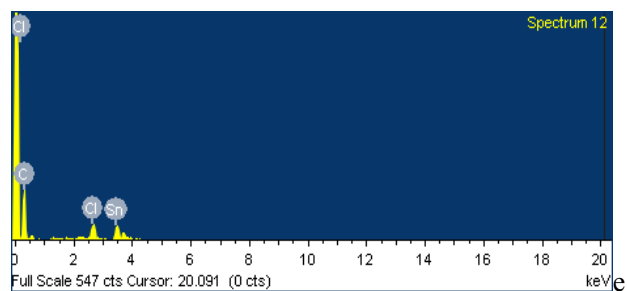
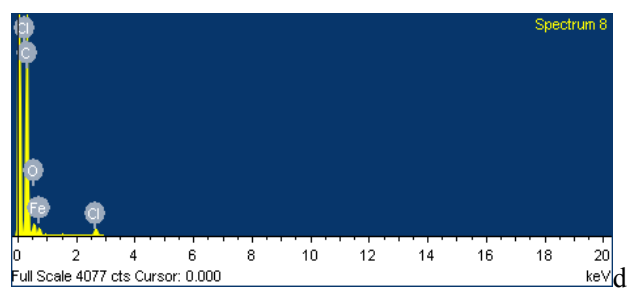
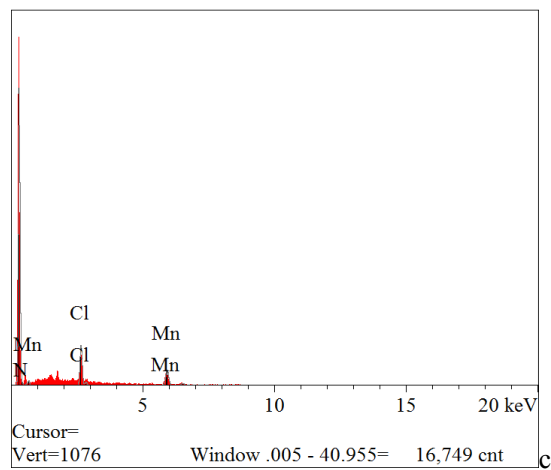
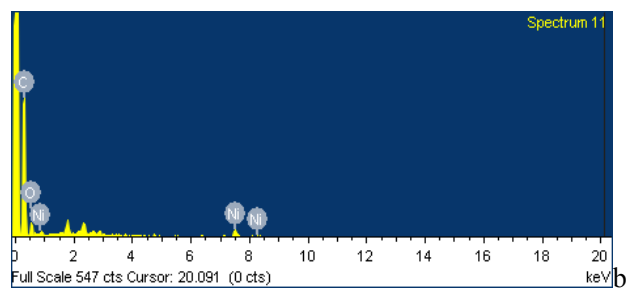
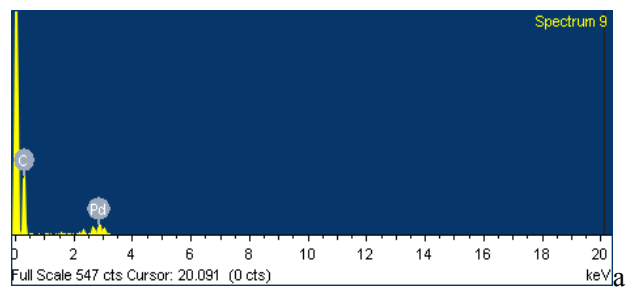


Figure S17. EDX spectra of a) Pd-tapp-A4, b) Ni-tapp-A4, c) Mn-tapp-A4, d) Fe-tapp-A4 and e) Sn-tapp-A4 aerogels. Quantitative values/atom%: a) Pd 5.96; b) Ni 1.56%; c) Mn 1.48, Cl 1.71; d) Fe 0.14, Cl 0.40; e) Sn 2.90, Cl 2.62.

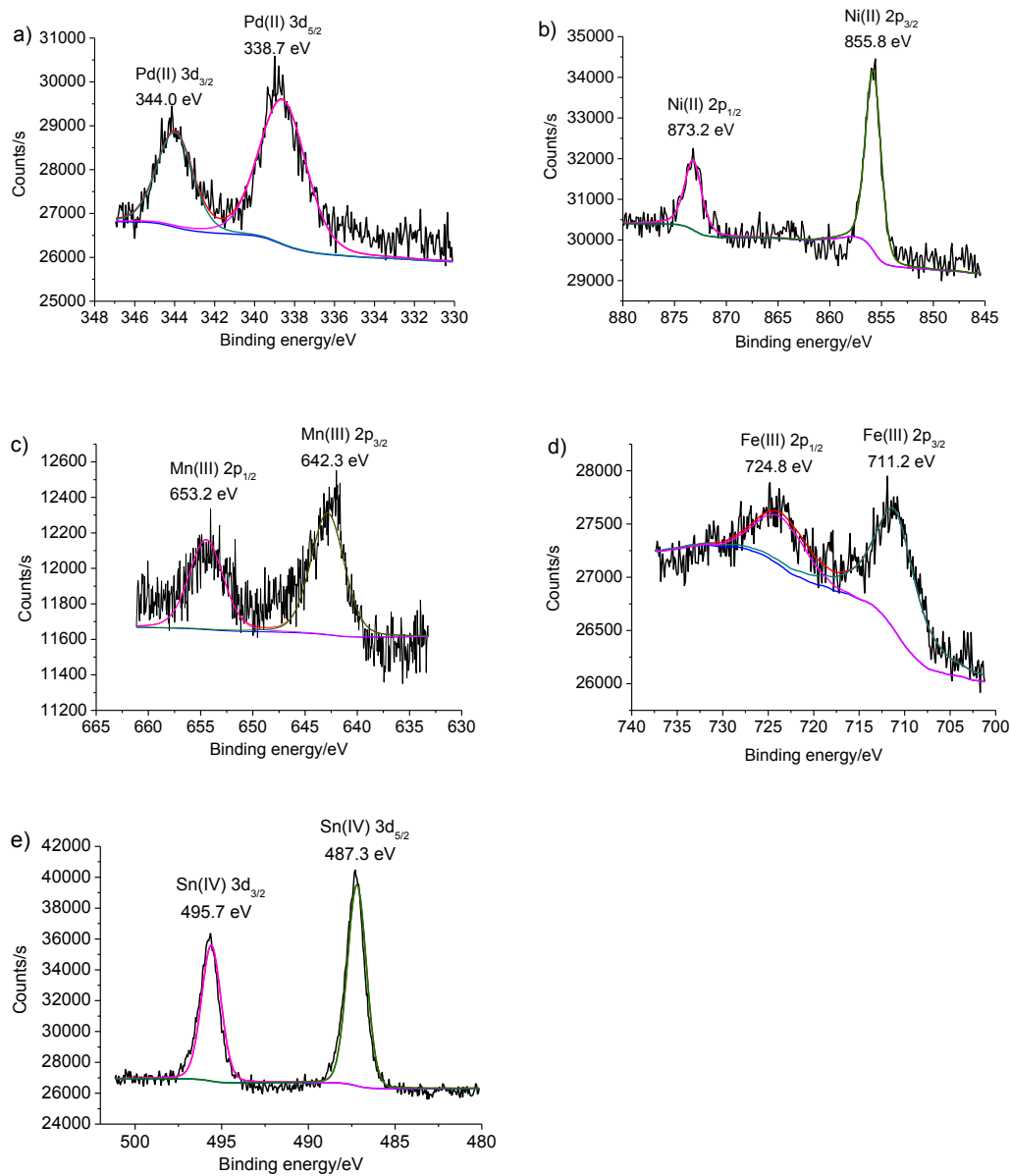


Figure S18. XPS and deconvoluted spectra a) Pd 3d for Pd-tapp-A4, b) Ni 2p for Ni-tapp-A4, c) Mn 2p for Mn-tapp-A4, d) Fe 2p for Fe-tapp-A4 and e) Sn 3d for Sn-tapp-A4.

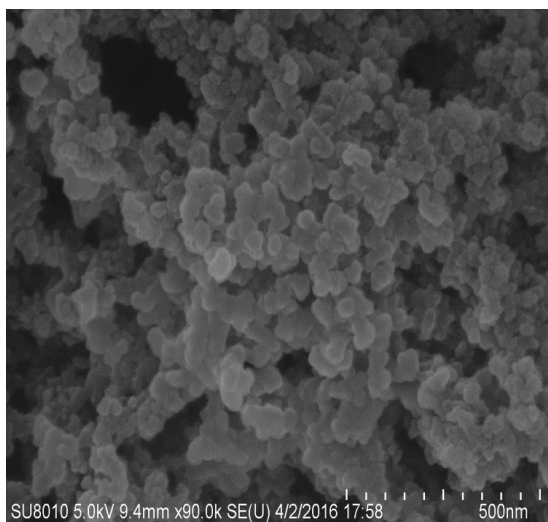


Figure S19. SEM image of H₂tapp-A4 aerogel that was immersed in 3 mol L⁻¹ NaOH solution overnight.

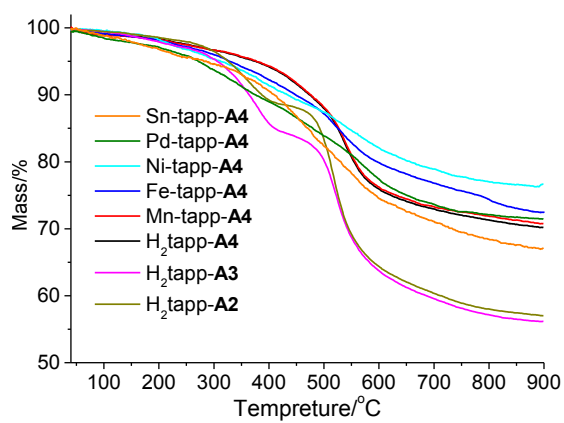


Figure S20. TG curves of H₂tapp-A2, H₂tapp-A3, H₂tapp-A4, Mn-tapp-A4, Fe-tapp-A4, Ni-tapp-A4, Pd-tapp-A4 and Sn-tapp-A4 aerogels.

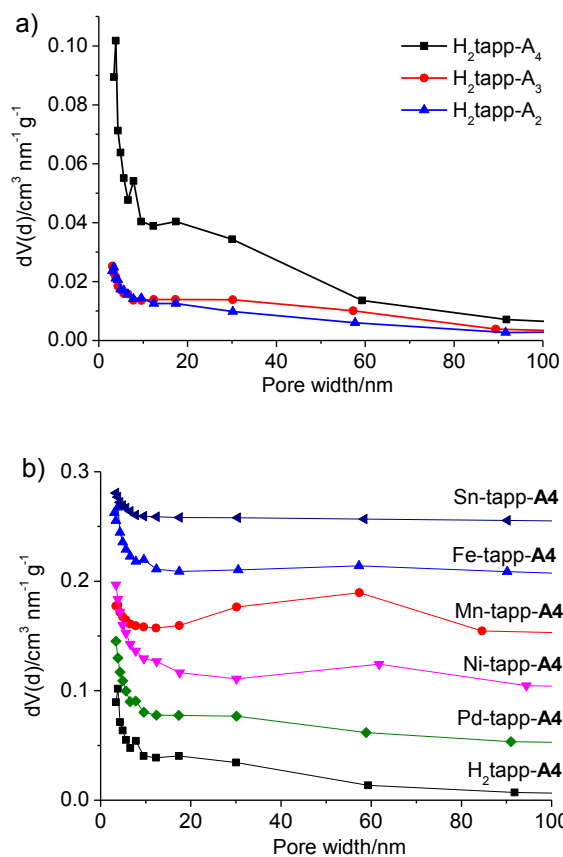


Figure S21. BJH pore size distributions of a) H_2 tapp-A₂, H_2 tapp-A₃ and H_2 tapp-A₄ aerogels, and b) H_2 tapp-A₄, Pd-tapp-A₄, Ni-tapp-A₄, Mn-tapp-A₄, Fe-tapp-A₄ and Sn-tapp-A₄ aerogels.

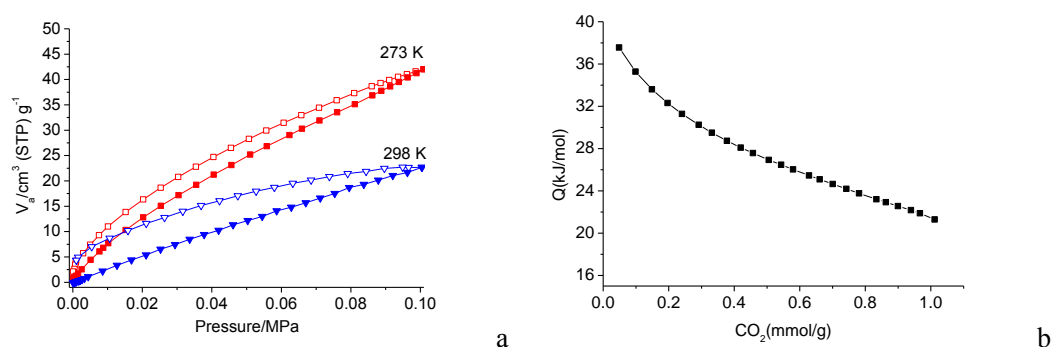


Figure S22. a) CO_2 adsorption-desorption isotherms of Ni-tapp-A₄ aerogel at 273 and 298 K, b) isosteric heats of adsorption (Q_{st}) as a function of gas loading.

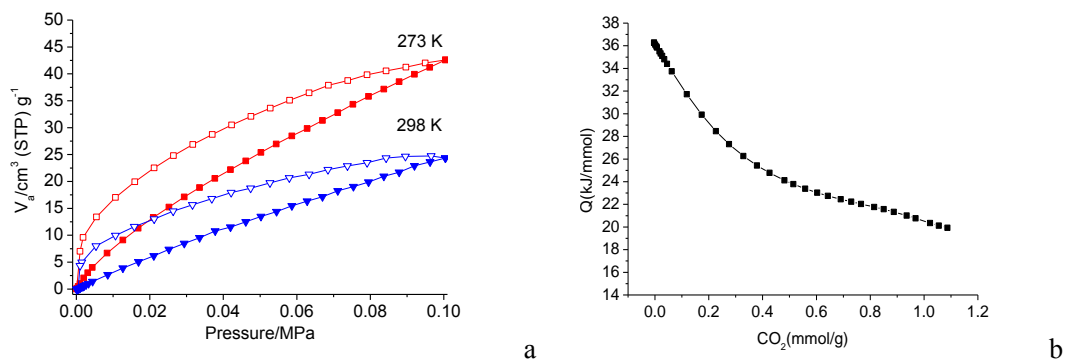


Figure S23. a) CO₂ adsorption-desorption isotherms of Mn-tapp-A4 aerogel at 273 and 298 K, b) isosteric heats of adsorption (Q_{st}) as a function of gas loading.

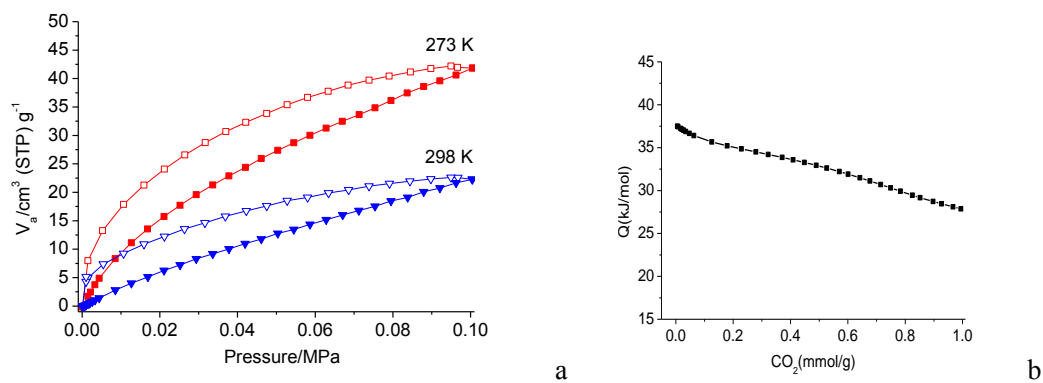


Figure S24. a) CO₂ adsorption-desorption isotherms of Fe-tapp-A4 aerogel at 273 and 298 K, b) isosteric heats of adsorption (Q_{st}) as a function of gas loading.

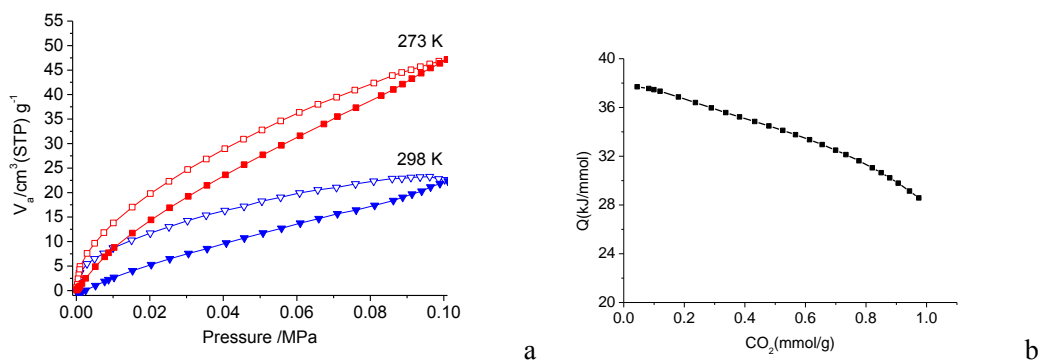


Figure S25 a) CO₂ adsorption-desorption isotherms of Sn-tapp-A4 aerogel at 273 and 298 K, b) isosteric heats of adsorption (Q_{st}) as a function of gas loading.

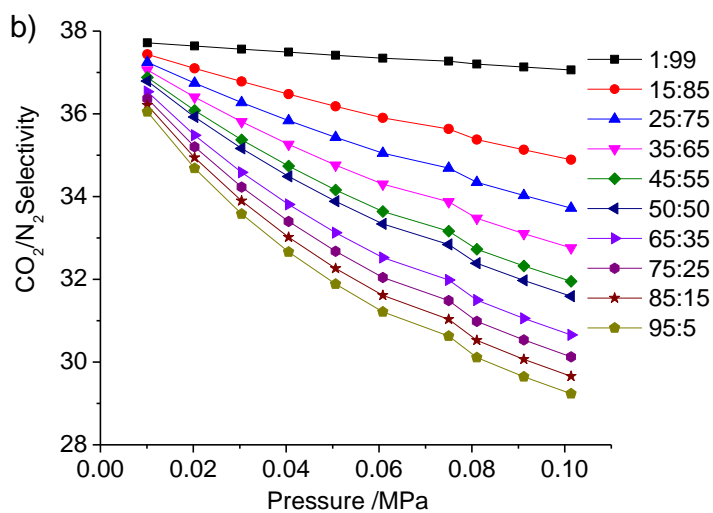
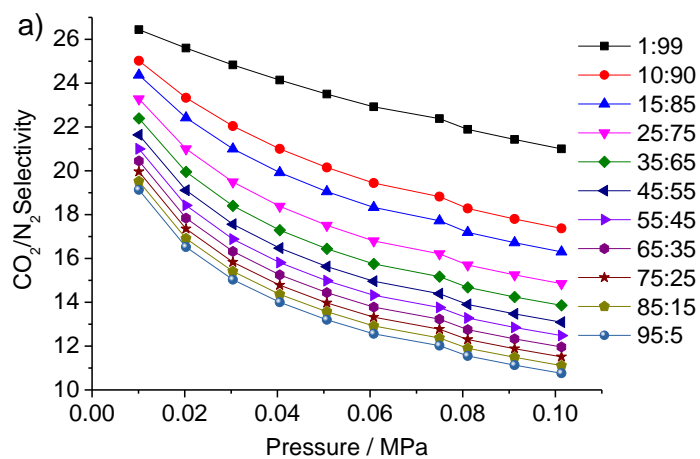


Figure S26. IAST selectivity of a) H₂tapp-A4 and b) Pd-tapp-A4 for CO₂/N₂ gas mixtures at 298 K.

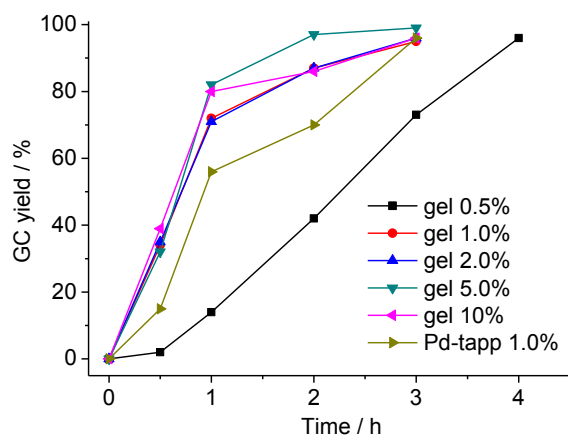


Figure S27. Suzuki-Miyaura reaction of 4-bromoanisole and phenylboronic acid catalyzed by Pd-tapp-A4 gel under batch conditions with various catalyst amounts and catalyzed by Pd-tapp under homogeneous conditions.